A wavelength tunable wavefront sensor for the human eye

Silvestre Manzanera, Carmen Canovas, Pedro M. Prieto* and Pablo Artal

Laboratorio de Optica, Universidad de Murcia (LOUM), Centro de Investigación en Óptica y Manofísica (CiOyN)
Edificio CiOyN, Campus de Espinardo, E-30071 Murcia (Spain)
**Corresponding author: pegrito@um.es*
http://lo.um.es

Abstract: We have designed and assembled an instrument for objective measurement of the eye's wave aberrations for different wavelengths with no modifications in the measurement path. The system consists of a Hartmann-Shack wave-front sensor and a Xe-white-light lamp in combination with a set of interference filters used to sequentially select the measurement wavelength. To show the capabilities of the system and its reliability for measuring at different wavelengths, the ocular aberrations were measured in three subjects at 440, 488, 532, 633 and 694 nm, basically covering the whole visible spectrum. Even for the shortest wavelengths, the illumination level was always several orders of magnitude below the safety limits. The longitudinal chromatic aberration estimates and the wavelength dependence of coma and spherical aberration, as examples of higher-order aberration terms, were compared to the predictions of a chromatic eye model, with good agreement. To our knowledge, this is the first report of a device to objectively determine the spectral fluctuations in the ocular wavefront.

OCIS codes: (330.0330) Vision, color, and visual optics; (010.7350) Wave-front sensing.

References and links

1. M. Tscherning, "Die monochromatischen Abberationen des menschlichen Auges," Z. Psychol. Physiol. Sinn. **6**, 456–471 (1894).
2. M. S. Smirnov, "Measurement of the wave aberration of the human eye," Biofizika **6**, 776-795 (1961).
3. B. Howland and H. C. Howland, "Subjective measurement of high-order aberrations of the eye," Science **193**, 580-582 (1976).
4. R. H. Webb, C. M. Penney, and K. P. Thompson, "Measurement of ocular local wavefront distortion with a spatially resolved refractometer," Appl. Opt. **31**, 3678-3686 (1992).
5. J. C. He, S. Marcos, R. H. Webb, and S. A. Burns, "Measurement of the wave-front aberration of the eye using a fast psychophysical procedure," J. Opt. Soc. Am. A **15**, 2449-2456 (1998).
6. P. M. Prieto, F. Vargas-Martin, J. S. McLellan, and S. A. Burns, "Effect of the polarization on ocular wave aberration measurements," J. Opt. Soc. Am. A **19**, 809-814 (2002).
7. R. H. Webb, C. M. Penney, J. Sobiech, P. R. Staver, and S. A. Burns, "SSR (Spatially Resolved Refractometer): A Null-Seeking Aberrometer," Appl. Opt. **42**, 736-744 (2003).
8. J. Z. Liang, B. Grimm, S. Goelz, and J. F. Bille, "Objective measurement of wave aberrations of the human eye with the use of a hartmann-shack wave-front sensor," J. Opt. Soc. Am. A **11**, 1949-1957 (1994).
9. J. Liang and D. R. Williams, "Aberrations and retinal image quality of the normal human eye," J. Opt. Soc. Am. A **14**, 2873-2883 (1997).
10. P. M. Prieto, F. Vargas-Martin, S. Goelz, and P. Artal, "Analysis of the performance of the Hartmann-Shack sensor in the human eye," J. Opt. Soc. Am. A **17**, 1388-1398 (2000).
11. G. Walsh, W. N. Charman, and H. C. Howland, "Objective technique for the determination of monochromatic aberrations of the human eye," J. Opt. Soc. Am. A **1**, 987-992 (1984).
12. R. Navarro and E. Moreno-Barriuso, "Laser ray-tracing method for optical testing," Opt. Lett. **24**, 951-953 (1999).
13. M. Mrochen, M. Kaemmerer, P. Mierdel, H. E. Krinke, and T. Seiler, "Principles of Tscherning aberrometry," J. Refract. Surg. **16**, S570-S571 (2000).
14. S. MacRae and M. Fujieda, "Slit Skiascopic-guided ablation using the Nidek laser," J. Refract. Surg. **16**, S576-S580 (2000).

#94180 - $15.00 USD Received 24 Mar 2008; revised 12 May 2008; accepted 13 May 2008; published 14 May 2008

15. I. Iglesias, R. Ragazzoni, Y. Julien, and P. Artal, "Extended source pyramid wave-front sensor for the human eye," Opt. Express **10**, 419-428 (2002), http://www.opticsexpress.org/abstract.cfm?URI=oe-10-9-419.
16. F. Diaz-Douton, J. Pujol, M. Arjona, and S. O. Luque, "Curvature sensor for ocular wavefront measurement," Opt. Lett. **31**, 2245-2247 (2006).
17. Y. U. Ogboso and H. E. Bedell, "Magnitude of lateral chromatic aberration across the retina of the human-eye," J. Opt. Soc. Am. A **4**, 1666-1672 (1987).
18. P. Simonet and M. C. W. Campbell, "The optical transverse chromatic aberration on the fovea of the human-eye," Vision Res. **30**, 187-206 (1990).
19. L. N. Thibos, A. Bradley, D. L. Still, X. Zhang, and P. A. Howarth, "Theory and measurement of ocular chromatic aberration," Vision Res. **30**, 33-49 (1990).
20. M. Rynders, B. Lidkea, W. Chisholm, and L. N. Thibos, "Statistical distribution of foveal transverse chromatic aberration, pupil centration, and angle-psi in a population of young-adult eyes," J. Opt. Soc. Am. A **12**, 2348-2357 (1995).
21. S. Marcos, S. A. Burns, E. Moreno-Barriuso, and R. Navarro, "A new approach to the study of ocular chromatic aberrations," Vision Res. **39**, 4309-4323 (1999).
22. S. Marcos, S. A. Burns, P. M. Prieto, R. Navarro, and B. Baraibar, "Investigating sources of variability of monochromatic and transverse chromatic aberrations across eyes," Vision Res. **41**, 3861-3871 (2001).
23. P. Artal, S. Marcos, R. Navarro, and D. Williams, "Odd aberrations and double-pass measurements of retinal image quality," J. Opt. Soc. Am. A **12**, 195- (1995).
24. A. Ames, Jr. and C. A. Proctor, "Dioptrics of the eye," J. Opt. Soc. Am. **5**, 22-84 (1921).
25. G. Wald and D. R. Griffin, "The change in refractive power of human eye in dim and bright light," J. Opt. Soc. Am. **37**, 321-336 (1947).
26. R. E. Bedford and G. Wyszecki, "Axial chromatic aberration of the human eye," J. Opt. Soc. Am. **47**, 564-565 (1957).
27. W. N. Charman and J. A. M. Jennings, "Objective measurements of the longitudinal chromatic aberration of the human eye," Vision Res. **16**, 999-1005 (1976).
28. P. A. Howarth, X. X. Zhang, A. Bradley, D. L. Still, and L. N. Thibos, "Does the chromatic aberration of the eye vary with age?," J. Opt. Soc. Am. A **5**, 2087-2092 (1988).
29. L. N. Thibos, M. Ye, X. Zhang, and A. Bradley, "The Chromatic Eye: a new reduced eye model of ocular chromatic aberration in humans," Appl. Opt. **31**, 3594-3600 (1992).
30. M. C. Rynders, R. Navarro, and M. A. Losada, "Objective measurement of the off-axis longitudinal chromatic aberration in the human eye," Vision Res. **38**, 513-522 (1998).
31. J. S. McLellan, S. Marcos, P. M. Prieto, and S. A. Burns, "Imperfect optics may be the eye's defence against chromatic blur," Nature **417**, 174-176 (2002).
32. A. Seidemann and F. Schaeffel, "Effects of longitudinal chromatic aberration on accommodation and emmetropization," Vision Res. **42**, 2409-2417 (2002).
33. Y. Benny, S. Manzanera, P. M. Prieto, E. N. Ribak, and P. Artal, "Wide-angle chromatic aberration corrector for the human eye," J. Opt. Soc. Am. A **24**, 1538-1544 (2007).
34. L. Llorente, L. Diaz-Santana, D. Lara-Saucedo, and S. Marcos, "Aberrations of the human eye in visible and near infrared illumination," Opt. Vis. Sci. **80**, 26-35 (2003).
35. E. J. Fernandez, A. Unterhuber, P. M. Prieto, B. Hermann, W. Drexler, and P. Artal, "Ocular aberrations as a function of wavelength in the near infrared measured with a femtosecond laser," Opt. Express **13**, 400-409 (2005), http://www.opticsexpress.org/abstract.cfm?URI=oe-13-2-400.
36. F. C. Delori and K. P. Pflibsen, "Spectral reflectance of the human ocular fundus," Appl. Opt. **28**, 1061-1067 (1989).
37. International Commission on Non-Ionizing Radiation Protection (ICNIRP), "Guidelines on limits of exposure to broad-band incoherent optical radiation (0.38 to 3 μm)," Health Phys. **73**, 539-554 (1997).
38. A. Guirao, P. Artal, "Corneal wave aberration from videokeratography: accuracy and limitations of the procedure," J. Opt. Soc. Am. A **17**, 955-965 (2000).

1. Introduction

Ocular aberrations degrade the retinal image and pose a limit to resolution both for vision and for retinal imaging. Two types of aberrations are typically described: monochromatic wave aberrations and chromatic aberrations. Wave aberrations come from differences in the optical path of rays entering or exiting through different pupil locations. They can emanate from irregularities both in the optical surfaces and in the refractive index distribution of the eye's components. This type of aberration affects the optical quality even in monochromatic light. Historically, distinction can be made between subjective [1-7] and objective [8-16] methods to measure the wave aberrations. Nowadays, practically all the systems in use correspond to the latter group and, among them, the Hartmann-Shack sensor [8-10] is virtually the standard.

Chromatic aberrations come from the dispersive nature of the ocular media and its negative effects on image quality should be apparent only in polychromatic light. Two types

#94180 - $15.00 USD Received 24 Mar 2008; revised 12 May 2008; accepted 13 May 2008; published 14 May 2008

of chromatic aberration are usually distinguished: transverse chromatic aberration (TCA) and longitudinal chromatic aberration (LCA). The TCA is defined as the lateral shift of the image as a function of wavelength. It has been widely studied in the literature [17-22], always using subjective measurement methods. In the fovea, it can be understood as a prism variation and, accordingly, it cancels out in double-pass [23]. As a consequence it seems difficult to devise an objective method to assess the foveal TCA. The LCA is the change with wavelength in the axial position of the focus and has been the subject of an extensive literature [19,21,24-33]. Defocus can be measured in double-pass and the LCA, unlike the TCA, can be objectively assessed. However, a vast majority of the reported LCA data, even in recent studies, has been obtained by means of subjective methods. The only exception, to our knowledge, is the double-pass method proposed by Charman and Jennings [27,30]. Also worth mentioning are the two-wavelength comparison between IR and visible [34] and the study in near IR using a femtosecond laser [35].

The foveal TCA and LCA can be understood as the dependence with wavelength of the lowest order terms of the wavefront. By analogy, higher order chromatic aberrations could be defined. As an historical precedent, Ames and Proctor [24] measured the spherical aberration for different wavelengths. However, only recently the chromatic variability of different wave aberration terms has been systematically studied. To our knowledge, only one device has been implemented until now to measure the wave aberrations for a set of wavelengths in the visible range: the modified spatially resolved refractometer [21,22,31], which is a subjective method. Additionally, Ref. [34] presents the two-wavelength comparison of aberration terms up to 7^{th} order in green and IR light. Finally, a recent study demonstrated the use of a Hartmann-Shack sensor to objectively determine the wavefront for a set of wavelengths in near IR [35].

In this work, we present a Hartmann-Shack-based apparatus to objectively measure the aberrations for a set of wavelengths in the visible range. A variation of this system was used to evaluate the optical quality of a recently proposed LCA-correcting device [33]. The procedure is similar and was developed in parallel to that presented in Fernandez et al [35]. In both cases, the procedure includes the use of a broad spectrum light source and a set of interference filters to tune the illumination wavelength without introducing further variations in the instrument. In this case, we use a Xenon white-light lamp that has a virtually flat spectrum in the visible range. To show the capabilities of the system, we have measured the wave aberrations in three subjects for five wavelengths (440, 488, 532, 633, and 694 nm), basically covering the visible range. It is important to note that filter availability is virtually the only constrain for wavelength selection. The chromatic dependence of defocus (i.e., the LCA), coma and spherical aberration, is compared to the predictions of the Indiana chromatic eye model [29] as an example of application.

2. Methods

2.1. Experimental apparatus

A schematic diagram of the apparatus is shown in Fig. 1. Wave-front sensing is performed by means of a Hartmann-Shack sensor. The main difference with respect to previous systems is the use of a Xenon white-light lamp (Hamamatsu L2274) as illumination source. The lamp spectrum is basically flat in the visible range from 400 to 800 nm. The measurement wavelength is selected by means of interchangeable interference filters inserted in front of the lamp housing. In this particular case, five 10-nm bandwidth (FWHM) filters were used, with peak transmittance at 440, 488, 532, 633 and 694 nm respectively. Although the lamp housing allows a certain degree of focusing, two lenses, L1 and L2, together with an aperture of 1-mm diameter, P1, are used to improve the quality of the beam entering the eye. A neutral density wedge, NF, is used to modify the intensity of the incoming beam. For each wavelength, the final intensity is a trade-off between the subject's comfort and the visibility of the H-S spots, always orders of magnitude below the safety limits. Finally, another 1-mm aperture, P2, limits the extent of the illumination beam to facilitate removing corneal reflections. The beam then

#94180 - $15.00 USD Received 24 Mar 2008; revised 12 May 2008; accepted 13 May 2008; published 14 May 2008

reaches the eye by means of beam splitter BS and its reflection on the retina acts as a pseudo-point source for measuring the eye's aberrations in the outward direction.

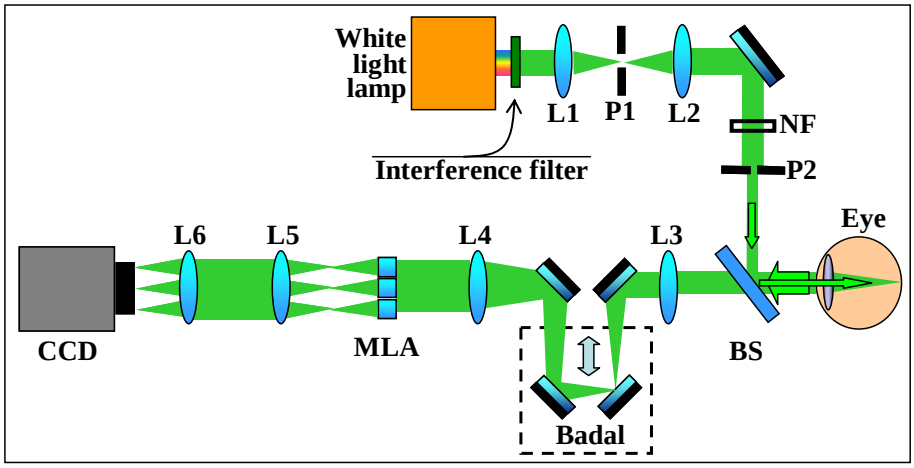

Fig. 1. Layout of the experimental apparatus. An H-S wave-front sensor is used to measure ocular aberrations. The light source is a white-light lamp and the measurement wavelength is selected by means of interchangeable interference filters. See the text for further details.

The light reflected in the retina is transmitted by the beam splitter and enters the measurement channel which, in its simplest version (see Fig. 1), consists of two lenses that optically conjugate the subject's pupil and the H-S microlens array, and a set of four mirrors (two of them fixed and two sliding) used to compensate the subject's defocus if necessary. For some applications, it is convenient to have intermediate pupil conjugate planes, which can be produced by introducing telescope-type lens assemblages before the microlens array. A mirror can be used to measure the system's intrinsic aberrations by introducing the collimated beam directly to the measurement channel without entering the eye. The subject's position is stabilized by means of a bite-bar mounted on a three axis stage. The pupil alignment is routinely checked on the spot image.

The dynamic range of the H-S sensor is primarily controlled by the numerical aperture of its microlens array. For this apparatus we selected a microlens pitch of 0.8 mm and a focal length of 8.2 mm to guarantee the measurement of the changes in defocus throughout the visible range. A unit-magnification telescope was used to optically relay the spot image onto the CCD plane. The camera was a cooled, monochrome Retiga 1300i (QImaging, Surrey, BC, Canada), specially designed for low light level applications. Designed to work in the visible range, the camera mounts from factory an IR filter to produce a broad spectral sensitivity peak around 500 nm. For the present application, we have removed the filter, thus increasing the camera sensitivity to the red part of the spectrum. As it will be discussed later, this allows a reduction in the required exposure time for long wavelengths.

2.2. Subjects and experimental procedure

The wave-front aberrations at the selected wavelengths (440, 488, 532, 633 and 694 nm) were measured in three young healthy subjects, EA (emmetrope, 24 yo), SM (2.75D myope, 32 yo), and VS (emmetrope, 22 yo). No cycloplegia was induced. For each experimental session, the initial pupil alignment was performed at the longest wavelength (694 nm), where the process is more comfortable for the subject due to the high reflectance-to-sensitivity ratio of the retina [36] and good quantum efficiency of the CCD chip.

#94180 - $15.00 USD Received 24 Mar 2008; revised 12 May 2008; accepted 13 May 2008; published 14 May 2008

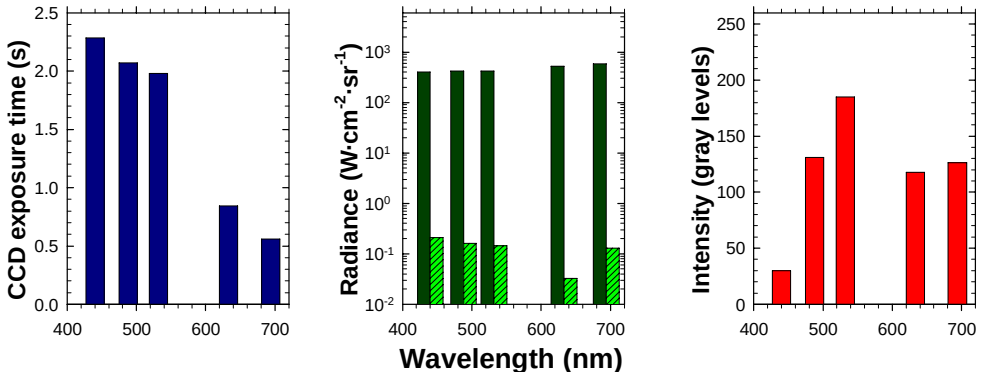

Fig. 2. Left: Exposure time settings. Center: Comparison between source radiance (light bars) and hazardous limits for incoherent sources (dark bars). Right: average spot intensity.

The wavelengths were selected sequentially by placing the corresponding interference filter in the holder. For each wavelength, the spot image intensity was adjusted by setting both the exposure time of the camera and the intensity of the illumination beam with the neutral density wedge. Figures 2-left and 2-center show the final values of exposure time and source radiance (at the pupil P1plane), respectively, as a function of wavelength. Especially for the longer wavelengths, attention was paid to the comfort and safety of the subject. As it can be seen in Fig. 2-center, the radiance was always several orders of magnitude below the hazardous limit [37]. The average spot intensity achieved for each wavelength is depicted in Fig. 2-right. When possible, the radiance and exposure time settings were selected to produce spot intensities around gray level 150 (8-bit depth). The exception to this rule was 440 nm: the poor quantum efficiency together with the tighter safety constraints would require an exposure time longer than feasible. Accordingly, the spot intensity for this wavelength can be seen lower than average. However, even in this case the spot pattern is clear enough to reliably process the H-S signal. For each wavelength and subject, a set of 4 images (6 images for 440 nm) were taken and the average Zernike coefficients were calculated over a 6-mm pupil. In all cases, the natural pupil was large enough for this analysis.

3. Results

The set of aberration maps for one of the subjects (EA) are shown in the top row of Fig. 3. Pupil size was 6 mm. Defocus has been arbitrarily set to 0 for 532 nm. Visually, the main feature in the aberration map for this wavelength is astigmatism, which is present in all the maps in the top row. In order to illustrate the spectral variations in the wavefront, the aberration map for 532 nm has been taken as reference and subtracted from each single-wavelength map to produce the central row in Fig. 3. As it would be expected, the main difference between wavelengths is defocus. To make this fact apparent, the bottom row in Fig. 3 shows the aberration maps after removing the individual defocus term for each wavelength from the maps in the central row. A similar behavior was found for the other two subjects. These results are in good agreement with the data from Marcos et al. [21], who found the higher order spectral fluctuations to be small.

As an example of application of the wavelength tunable wavefront sensor, we have compared the spectral behavior of selected aberration terms with the predictions of the Indiana chromatic model eye. To study the longitudinal chromatic aberration, the Seidel defocus term was calculated using 2nd and 4th order Zernike coefficients [38], and translated into diopters. 532-nm was taken as reference wavelength and, consequently, defocus for this wavelength was subtracted from each subject's series. Figure 4 shows the individual and mean defocus values. These values can be compared to the predictions of the Indiana model eye, shifted to produce 0-D defocus for 532 nm, with good agreement between experiment and theory.

#94180 - $15.00 USD Received 24 Mar 2008; revised 12 May 2008; accepted 13 May 2008; published 14 May 2008

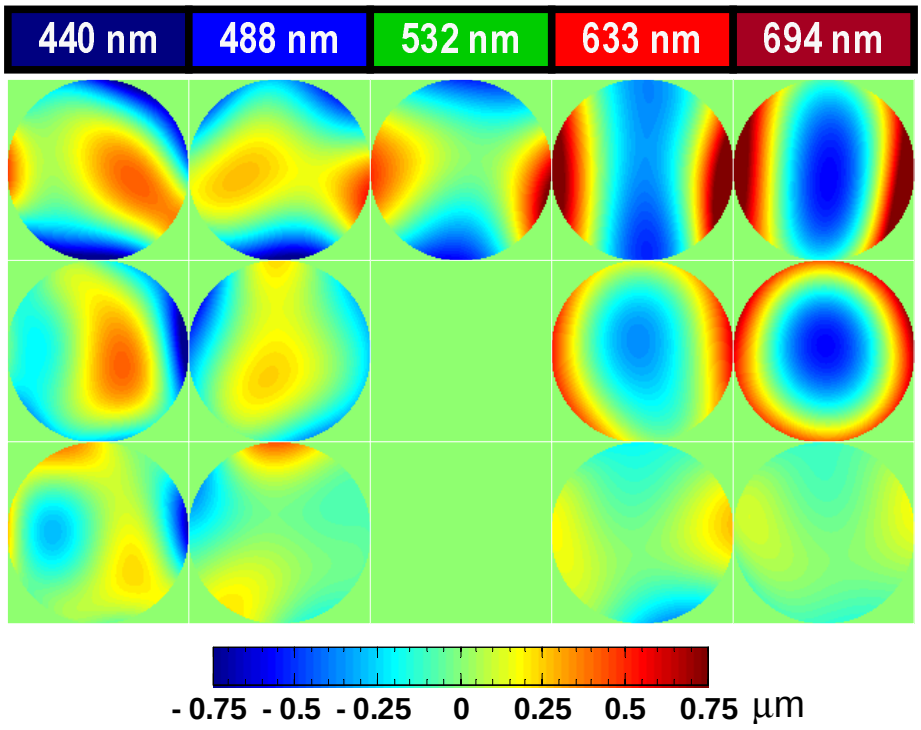

Fig. 3. Wavefront chromatic differences for subject EA. Top row: WA for each wavelength, including the defocus term, which has been arbitrarily set to 0 for 532 nm. Central row: Difference between the WA for each wavelength and the WA for 532 nm, arbitrarily taken as reference. Bottom row: higher order chromatic fluctuations obtained by removing the individual defocus term from each WA map in the central row. Pupil size was 6 mm.

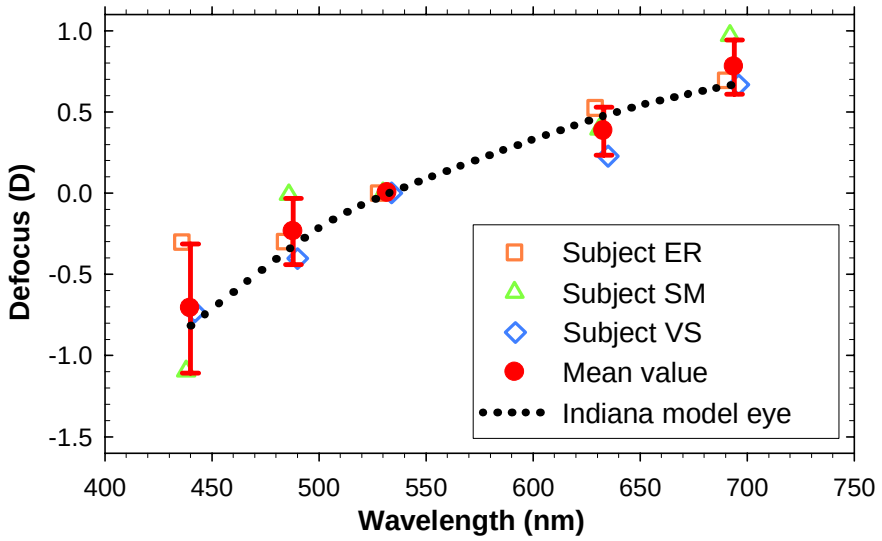

Fig. 4. LCA estimates calculated as differences in focus with respect to 532 nm. Open symbols: individual values. Solid circles: mean values, with the standard deviation as error bar. Dotted line: Indiana model eye predictions shifted to cancel out the defocus for 532 nm.

#94180 - $15.00 USD Received 24 Mar 2008; revised 12 May 2008; accepted 13 May 2008; published 14 May 2008

Finally, Figs. 5 and 6 show spherical aberration and vertical coma, selected as examples of radially symmetric and asymmetric aberrations respectively. Again, the aberration values are referred to the 532-nm ones. In both cases, the spectral behavior of the aberrations agrees with the chromatic eye model. Spherical aberration shows a minor increase with wavelength while vertical coma remains basically constant as predicted, in both cases, by the eye model. Once again, this behavior compares well with the results in Ref. [21].

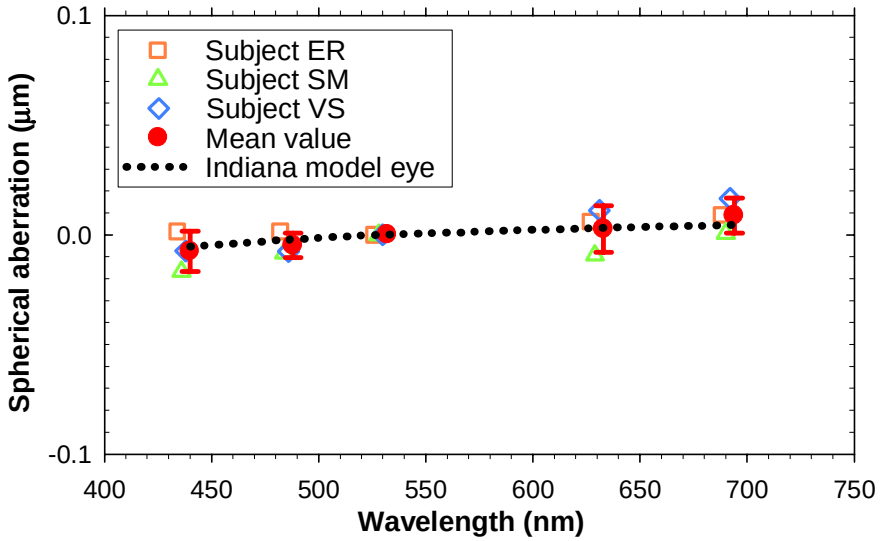

Fig. 5. Chromatic differences in spherical aberration for a 6-mm pupil. Reference wavelength was 532 nm. Open symbols: individual values. Solid circles: mean values, with standard deviation as error bar. Dotted line: Indiana model eye predictions shifted to cancel out the spherical aberration for 532 nm.

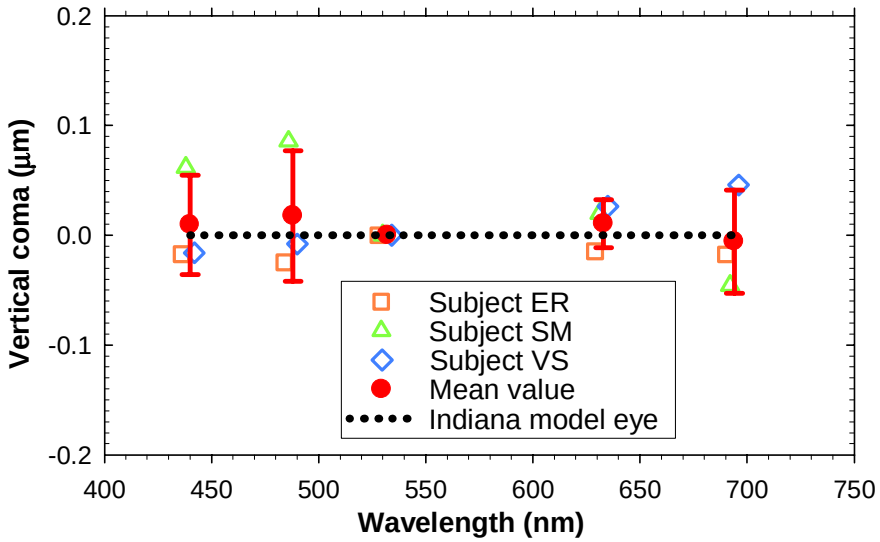

Fig. 6. Chromatic differences in vertical coma for a 6-mm pupil. Reference wavelength was 532 nm. Open symbols: individual values. Solid circles: mean values, with the standard deviation as error bar. Dotted line: Indiana model eye predictions.

#94180 - $15.00 USD Received 24 Mar 2008; revised 12 May 2008; accepted 13 May 2008; published 14 May 2008

4. Conclusions

We present here a wavelength tunable wavefront sensor that allows easy and fast wavelength switching without changes in the measurement path. The main difference with respect to previous systems lies in the illumination source: A Xenon white-light lamp, with a virtually flat spectrum across the visible, is used in combination with interchangeable interference filters to select the measurement wavelength. The system can be used to objectively study the chromatic fluctuations of the ocular aberrations, including the longitudinal chromatic aberration. As an example of use, we have measured the aberrations for five wavelengths in three subjects and compared the results with the predictions of the Indiana chromatic eye model, with good agreement in all cases. The device presented here can be a useful tool to refine chromatic eye models, to develop and study chromatic aberration correctors or to include the chromatic effects in the optimization procedures of new ophthalmic optics elements.

Acknowledgments

This work has been supported in part by the Ministerio de Educación y Ciencia of Spain, grants FIS2004-2153, FIS2007-64765, CIT-020500-2005-031, CIT-020400-2007-64; and Fundación Seneca (Region de Murcia, Spain), grant 4524/GERM/06.

#94180 - $15.00 USD Received 24 Mar 2008; revised 12 May 2008; accepted 13 May 2008; published 14 May 2008